University of Massachusetts Medical School

eScholarship@UMMS

Cancer Biology Publications and Presentations

Molecular, Cell and Cancer Biology

2013-10-01

Id2 complexes with the SNAG domain of Snai1 inhibiting Snai1-mediated repression of integrin beta4

Cheng Chang
University of Massachusetts Medical School

Et al.

Let us know how access to this document benefits you.

Follow this and additional works at: https://escholarship.umassmed.edu/cancerbiology_pp

Part of the Amino Acids, Peptides, and Proteins Commons, Cancer Biology Commons, Cell Biology Commons, Developmental Biology Commons, Molecular Biology Commons, and the Neoplasms Commons

Id2 Complexes with the SNAG Domain of Snai1 Inhibiting Snai1-Mediated Repression of Integrin β4

Cheng Chang, Xiaofang Yang, Bryan Pursell, Arthur M. Mercurio

University of Massachusetts Medical School, Worcester, Massachusetts, USA

The epithelial-mesenchymal transition (EMT) is a fundamental process that underlies development and cancer. Although the EMT involves alterations in the expression of specific integrins that mediate stable adhesion to the basement membrane, such as α6β4, the mechanisms involved are poorly understood. Here, we report that Snai1 inhibits β4 transcription by increasing repressive histone modification (trimethylation of histone H3 at K27 [H3K27Me3]). Surprisingly, Snai1 is expressed and localized in the nucleus in epithelial cells, but it does not repress β4. We resolved this paradox by discovering that Id2 complexes with the SNAG domain of Snai1 on the β4 promoter and constrains the repressive function of Snai1. Disruption of the complex by depleting Id2 resulted in Snai1-mediated β4 repression with a concomitant increase in H3K27Me3 modification on the β4 promoter. These findings establish a novel function for Id2 in regulating Snai1 that has significant implications for the regulation of epithelial gene expression.

The regulated expression of specific integrins is a fundamental component of development, tissue homeostasis, and many diseases (1). A prime example of this concept is the regulation of epithelial integrins, which function primarily in the anchoring of epithelial cells to laminins in the basement membrane (2). Developmental and pathological processes that necessitate epithelial cell migration often involve disruption of the stable adhesive contacts provided by integrins (3–5). The two major integrins that anchor epithelial cells to basement membrane laminins are α3β1 and α6β4 (6–9), and stimuli that disrupt epithelial adhesion frequently target the expression, localization, and cytoskeletal interactions of α6β4 (3, 4, 10–12). The epithelial-mesenchymal transition (EMT) provides a useful model system for studying the regulation of epithelial integrins. Although studies on the EMT have focused largely on mechanisms that disrupt cell-cell adhesions (13, 14), disruption of integrin-mediated anchoring to matrix is an important component of the EMT, but the mechanisms involved are poorly understood.

The EMT of normal mammary epithelial cells involves transcriptional repression of the β4 integrin subunit (referred to as β4), which results in loss of the α6β4 integrin (15). This repression is associated with a decrease in active histone modifications (acetylation of histone H3 at K9 [H3K9Ac] and trimethylation of histone H3 at K4 [H3K4Me3]) and an increase in repressive histone modification (H3K27Me3) on the β4 promoter (15). Although these previous observations provide a foundation for understanding how β4 is regulated during the EMT, little is known about the mechanisms involved. For example, are specific transcription factors involved in β4 repression, and, if so, what is their relationship to epigenetic modifications? Our pursuit of this problem in the current study revealed a key role for the zinc finger protein Snai1 in repressing β4. Interestingly, however, we observed that Snai1 is expressed in the nucleus of mammary epithelial cells, but it does not repress β4 transcription. This observation is consistent with other reports of Snai1 expression in epithelial cells (16–18). Aside from the possibility that Snai1 can be excluded from the nucleus (19), it is not known why nuclear Snai1 does not repress genes in epithelial cells. In an attempt to understand this paradox, we discovered that Snai1 interacts with Id2, and we demonstrate that Id2 constrains the repressive function of Snai1 by binding to its SNAG domain, a key domain for recruiting corepressors, including H3K27 methyltransferase (20). Id2 is a helix-loop-helix (HLH) protein family member that has been implicated as an antagonist of the EMT (21, 22). Specifically, the EMT in several epithelial models is associated with strong suppression of Id2, and forced Id2 expression in mesenchymal cells is able to partially rescue an epithelial phenotype (21). Given that Id2 can also impede the ability of Snai1 to repress E-cadherin, these findings provide insight into the regulation of epithelial genes, and they identify a novel mechanism for how Id2 maintains epithelial differentiation.

MATERIALS AND METHODS

Cell culture. NMuMG (normal murine mammary gland) cells were purchased from ATCC and maintained in complete medium containing Dulbecco's modified Eagle's medium (DMEM) (high glucose) with 10% fetal bovine serum, 10 μg/ml insulin, 100 μg/ml streptomycin, and 100 units/ml penicillin at 37°C in an incubator supplied with 5% CO_2. Transforming growth factor β (TGF-β; Peprotech) was added directly into the culture medium at a final concentration of 4 ng/ml for the time periods indicated in the figure legends. For long-term (more than 2 days) treatment with TGF-β (EMT), cells were passed into fresh complete medium containing 4 ng/ml TGF-β. For the TGF-β withdrawal experiments, cells that had undergone EMT in the presence of TGF-β were passed into fresh complete medium without TGF-β. MCF7 cells were purchased from ATCC and maintained in the DMEM (low glucose) containing 10% fetal bovine serum, 100 μg/ml streptomycin, and 100 units/ml penicillin at 37°C in an incubator supplied with 5% CO_2.

Microarray analysis. A Qiagen RNeasy minikit was used to extract total RNA from untreated epithelial NMuMG cells (EPTH), NMuMG cells treated with TGF-β for 11 days (EMT), and NMuMG cells treated with TGF-β for 11 days followed by TGF-β withdrawal for 13 days (mesenchymal-epithelial transition [MET]). For each sample, 500 ng of total RNA with poly(A) RNA control stock was used to synthesize the biotin-labeled antisense RNA (aRNA), following the protocol described in the manual of the Affymetrix 3′ IVT Express Kit (23). The aRNA was then purified using aRNA-binding magnetic beads and fragmented to a size range of 90 to 110 nucleotides (nt). The purified aRNA (15 μg) was used to hybridize with the Mouse Genome 430 2.0 Array (Affymetrix). All samples were run in duplicate. Analyses were performed using BRB-ArrayTools developed by Richard Simon and the BRB-ArrayTools Development Team (24). The raw array data were normalized using the robust multiarray average (RMA) algorithm. The three sample groups described above were subjected to class comparison, and genes that were differentially expressed are summarized in the Venn diagram shown in Fig. S1A in the supplemental material. Genes that exhibited less than a 2-fold change or a P value of >0.001 were excluded from the data summary presented.

Biochemical techniques. For quantitative, real-time PCR (qPCR), total RNA was extracted using TRIzol reagent (Invitrogen), and cDNAs were produced using Superscript II (Invitrogen) according to the manufacturer's instructions. qPCR was performed using a SYBR green master mix (Applied Biosystems). The qPCR primers used are provided in Table S1 in the supplemental material. Two-tailed Student t tests were used for statistical comparison. Immunoblotting was performed as described previously (25) using antibodies (Abs) for the following: β4 (505) (11), actin (A20660; Sigma), E-cadherin (334000; Invitrogen), Id2 (C-20; Santa Cruz Biotechnology), Id1 (C-20; Santa Cruz Biotechnology), Snai1 (L70G2; Cell Signaling), Pol2 (8WG16; Covance), Flag (M2; Sigma), and hemagglutinin (HA) (clone 3F10; Roche). Densitometry of the immunoblots was performed using Gel-pro Analyzer, version 4.0.

The nuclear fraction assay used is described in the Abcam protocol database (http://www.abcam.com/index.html?pageconfig=resource&rid=11408). Briefly, cells were extracted using buffer A (10 mM HEPES, 1.5 mM MgCl₂, 10 mM KCl, 0.5 mM dithiothreitol [DTT], 0.05% NP-40, pH 7.9) and centrifuged at 800 × g at 4°C for 10 min. The supernatant from this extract was saved as the cytoplasmic fraction. The remaining pellets were Dounce homogenized, extracted using buffer B (5 mM HEPES, 1.5 mM MgCl₂, 0.2 mM EDTA, 0.5 mM DTT, 26% glycerol [vol/vol], pH 7.9) containing 300 mM NaCl and centrifuged at 16,100 × g for 20 min at 4°C. The supernatant from this extraction was saved as the nuclear fraction.

For the coimmunoprecipitation (co-IP) experiments, cell extracts were prepared using NP-40 or Triton lysis buffer (Boston BioProduct) containing protease inhibitor cocktail (Roche). Extracts were precleared using a 50% protein G suspension (Biovision). For each IP, 200 to 500 μg of total protein was incubated with 40 μl of anti-Flag (M2) bead slurry (Sigma) at 4°C overnight in the appropriate lysis buffer. In some experiments, total protein was incubated with 1 μg of antibody overnight at 4°C first and then subjected to bead enrichment by 40 μl of 50% protein G slurry (Biovision) for another 1 to 2 h at 4°C. Subsequently, beads were washed with 1 ml of cold IP lysis buffer, and immunoprecipitated fractions were extracted by boiling in 2× SDS loading buffer (Boston Bioproducts). Samples were then resolved by SDS-PAGE and immunoblotted. IP antibodies were Snai1 Ab1 (L70G2; Cell Signaling), Snai1 Ab2 (G-7; Santa Cruz Biotechnology), and HA (clone 3F10; Roche).

Constructs, transfections, and RNA interference. pCMX-based expression constructs including HA alone, HA-Snai1 (mouse), or Flag-Id2 (mouse) were inserted between the KpnI-BamHI sites of the pCMX vector. PT7CFE1-based expression constructs, PT7CFE1-Id2 and PT7CFE1-Id1 (mouse), were cloned between NdeI and NotI sites of the PT7CFE1-CHis vector (Thermo Fisher Scientific). To construct the luciferase reporter for the β4 promoter, promoter fragments from −1572 to +254 were amplified by PCR using a KOD high-fidelity DNA polymerase kit (Novagen). Each fragment was gel purified by a Qiagen gel extraction kit,

digested with restriction enzymes (NEB), and inserted between the NheI and HindIII sites into the pGL3-basic vector (Promega). All constructs were confirmed by sequencing analysis (Genewiz).

Retrovirus-mediated expression in NMuMG cells was performed using the MSCV-IRES-GFP vector (where MSCV is murine stem cell virus, IRES is internal ribosome entry site, and GFP is green fluorescent protein) (plasmid 9044 [Addgene], also termed pMIG), and stable expression was confirmed by assessing GFP-positive cells, which comprised 90 to 100% of the cell population. The full-length Snai1 (mouse) open reading frame (ORF) was PCR amplified from the total cDNA of NMuMG cells and ligated into pMIG. To construct Snai1-ΔSNAG, the Snai1 (mouse) ORF lacking the 4th to 60th nucleotides was generated by PCR and ligated into pMIG. An HA tag was added on the 3′ end of Snai1 or the Snai1-ΔSNAG ORF to produce Snai1-HA or Snai1-ΔSNAG-HA. All cDNAs were inserted between XhoI and NotI sites of pMIG.

To construct glutathione S-transferase (GST)–SNAG and GST-Snai1, the SNAG domain (nt 1 to 60 of *Mus* Snai1) or the full-length Snai1 (mouse) ORF was cloned into the EcoRI site of the PGEX4T-1 vector (GE Healthcare). For GST-Id2, the full-length Id2 ORF was PCR amplified and then cloned into the pGEX-4T-1 vector with BamHI/SalI restriction sites. All constructs were confirmed by sequencing analysis (Genewiz).

The inducible system using an estrogen receptor (ER) fusion protein has been described previously (26–28). The retroviral Snai1-ER expression construct, PWZL-Snai1-ER (referred to as Snail-ER), was provided by Karl Simin (University of Massachusetts Medical School). The construction of the vector is described elsewhere (29). NMuMG cells infected by Snai1-ER virus were selected by blasticidin (6 μg/ml) for 7 days. All of the blasticidin-resistant NMuMG cells with Snai1-ER stable integration were then treated with medium containing 250 nM 4-hydroxytamoxifen (4-OHT) for Snai1 activation or an equal volume of ethanol (the solvent of 4-OHT) as a control for 7 days prior to protein analysis.

The constructs expressing the short hairpin RNA (shRNA) targeting Snai1 (shSnai1) were generated using Psuperior-Neo retroviral vector (Oligoengine). The shRNA targeting sequences are GGGAGAAAGATGTTTACAT (shSnai1-2) and CACCTTCTTTGAGGTACAA (shSnai1-3). Stable expression of these shRNAs in the NMuMG cells was obtained by G418 (1 mg/ml) selection for 7 days after retroviral infection, using shGFP as a nontargeting control. The mouse and human shId2 expression constructs used in this study were purchased from Open Biosystems, and the reference numbers are as follows: mouse shId2-1, TRCN0000054390, and shId2-2, TRCN0000054391; human shId2-1, TRCN0000021064, and shId2-2, TRCN0000021065. Stable expression of these pLKO-based vectors in NMuMG cells was obtained by puromycin (2 μg/ml) selection for 5 to 6 days, using shGFP as a nontargeting control.

ChIP. Chromatin immunoprecipitation (ChIP) assays were performed using a ChIP-it Express Kit (catalog number 53008; Active Motif) with minor modifications according to Tian et al. (30). Cells were first cross-linked with 2 mM disuccinimidyl glutarate (catalog number c1104; Proteochem) for 45 min at room temperature (RT) and then washed and subjected to cross-linking by 1% formaldehyde (Sigma) for 15 min at RT. The reaction was quenched using 125 mM glycine for 5 min. Subsequently, the cells were washed with phosphate-buffered saline (PBS), scraped from the plate, and lysed in 1 ml of lysis buffer [5 mM piperazine-$N,N′$-bis(2-ethanesulfonic acid) (PIPES; pH 8.0), 85 mM KCl, 0.5% NP-40, and protease inhibitor]. Nuclear pellets were lysed again with nuclear fraction buffer (50 mM Tris-HCl, 10 mM EDTA, 1% SDS, pH 8.0, and protease inhibitor) and resuspended in 400 μl of ChIP buffer (150 mM NaCl, 50 mM Tris-HCl, 1 mM EDTA, 1% Triton X-100, 0.1% sodium deoxycholate, 0.1% SDS with protease inhibitor). Chromatin was then subjected to sonication using a Sonicator 3000 (Misonix, Inc.) for four cycles of 20-s (power setting, 2.0) bursts to generate chromatin fragments that ranged from 200 to 700 bp. The sonicated chromatin samples were then used in the ChIP assay according to the protocol of the kit. Each ChIP sample contained chromatin from 1 × 10⁶ to 2 × 10⁶ cells and 2 μg of Ab. For ChIP, antibodies for the following were used: H3K27Me3 (07-449;
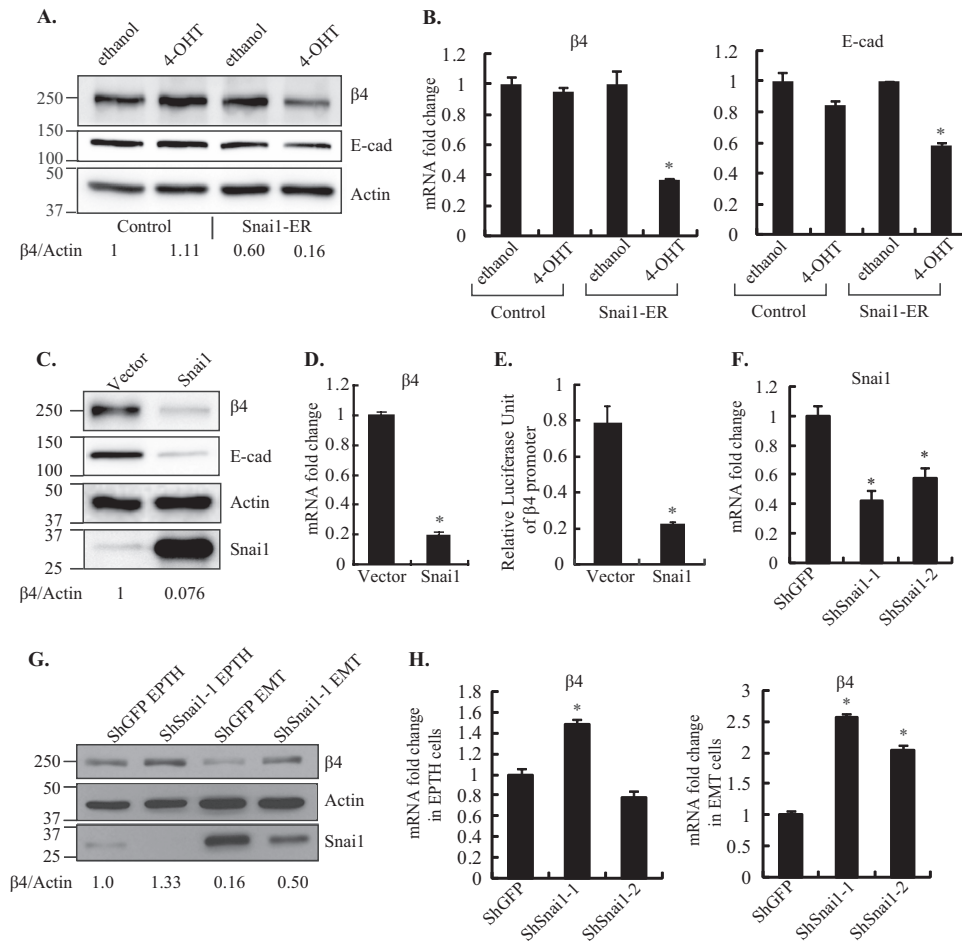
FIG 1 Snai1 represses β4 integrin. (A) NMuMG cells that stably express either a control ER construct or a Snai1-ER construct were treated with either 250 nM 4-OHT or an equal volume of ethanol (solvent) for 7 days. Subsequently, expression of β4, E-cadherin (E-cad), and actin was assessed by immunoblotting. Numbers below the blots indicate relative intensity of the bands based on densitometry (same as below). (B) Expression of β4 and E-cadherin mRNAs was quantified by qPCR in the same populations as described in panel A. *, $P < 0.05$. (C to E) Snai1 cDNA or empty vector was expressed in NMuMG cells, and the expression of β4, E-cadherin, Snai1, and actin was evaluated by immunoblotting (C), and β4 mRNA expression was quantified by qPCR (D) (*, $P < 0.05$). The relative luciferase activity of the β4 promoter in the control and Snai1-expressing cells was determined (E) (*, $P < 0.05$). (F) Snai1 expression in NMuMG cells was stably diminished using two independent shRNAs, and the effect was quantified by qPCR. (G) The control and Snai1 knockdown cells described in panel F were treated with either carrier (EPTH) or TGF-β (EMT) for 2 days to induce an EMT, and the expression of β4, Snai1, and actin was assessed by immunoblotting (G). (H) The expression of β4 mRNA in the control or shSnai1 NMuMG cells with the same treatment as described in panel G was quantified by qPCR (*, $P < 0.05$). Numbers on the left of the blots indicate the size (in kilodaltons) of the protein standard.

Millipore), H3K4Me3 (05-1339; Millipore), H3K9Me3 (07-442; Millipore), and H3 (2650; Cell signaling). Snai1 ChIP-grade Ab was a kind gift of A. de Herreros (31); Id2 (clone C-20; Santa Cruz Biotechnology) or isogenic IgG was used. ChIP incubation was performed overnight (15 h to 16.5 h) at 4°C. The immunoprecipitated DNA was then subjected to real-time PCR analysis using ChIP primers targeting different regions of the β4 promoter. Primer sets for ChIP PCR on the β4 promoter are provided in Table S1 in the supplemental material. Two-tailed Student *t* tests were used for statistical comparison.

Immunofluorescence microscopy. Immunofluorescence microscopy was performed as described previously (10) using Snai1 Ab (1:50 dilution) (L70G2; Cell Signaling) and Id2 Ab (1:200 dilution) (C-20; Santa Cruz Biotechnology), anti-mouse tetramethyl rhodamine isocyanate (TRITC) secondary Ab (1:250 dilution) (15-025-150; Jackson ImmunoResearch) and anti-rabbit fluorescein isothiocyanate (FITC)-secondary Ab (1:250 dilution) (711-096-152; Jackson ImmunoResearch). The microscope was made by Zeiss (model LSM-700), and the pictures were taken using the camera of an Axio Imager Z2 at room temperature

(23°C). A 40× oil immersion objective with a numerical aperture of 1.30 was used. The pictures were analyzed and exported using ZEN 2011 and processed using Adobe Photoshop.

Luciferase reporter assays. NMuMG cells were grown in 24-well plates and transiently transfected with 0.5 μg of each reporter construct and 0.1 μg of *Renilla* luciferase using 2 μl of Lipofectamine 2000 in 100 μl of Opti-MEM mix for each well. Luciferase assays were performed using a Dual-Luciferase reporter assay System (Promega). All experiments were performed in triplicate. Promoter activity was reported as the average of the ratio of firefly luciferase to *Renilla* luciferase. Two-tailed Student *t* tests were used for statistical comparison.

GST pulldown experiments. The methods for GST purification and the GST pulldown assay have been described elsewhere (32). Briefly, GST constructs were expressed in *Escherichia coli* strains JM109 or BL21(DE3) with isopropyl-β-D-thiogalactopyranoside (IPTG; 100 μM) stimulation for 3 h at 37°C. Cells were then lysed, and the GST fusion proteins were purified using glutathione-Sepharose 4B (Bioworld). The molecular mass of the purified GST fusion protein was confirmed by SDS-PAGE. *In vitro*
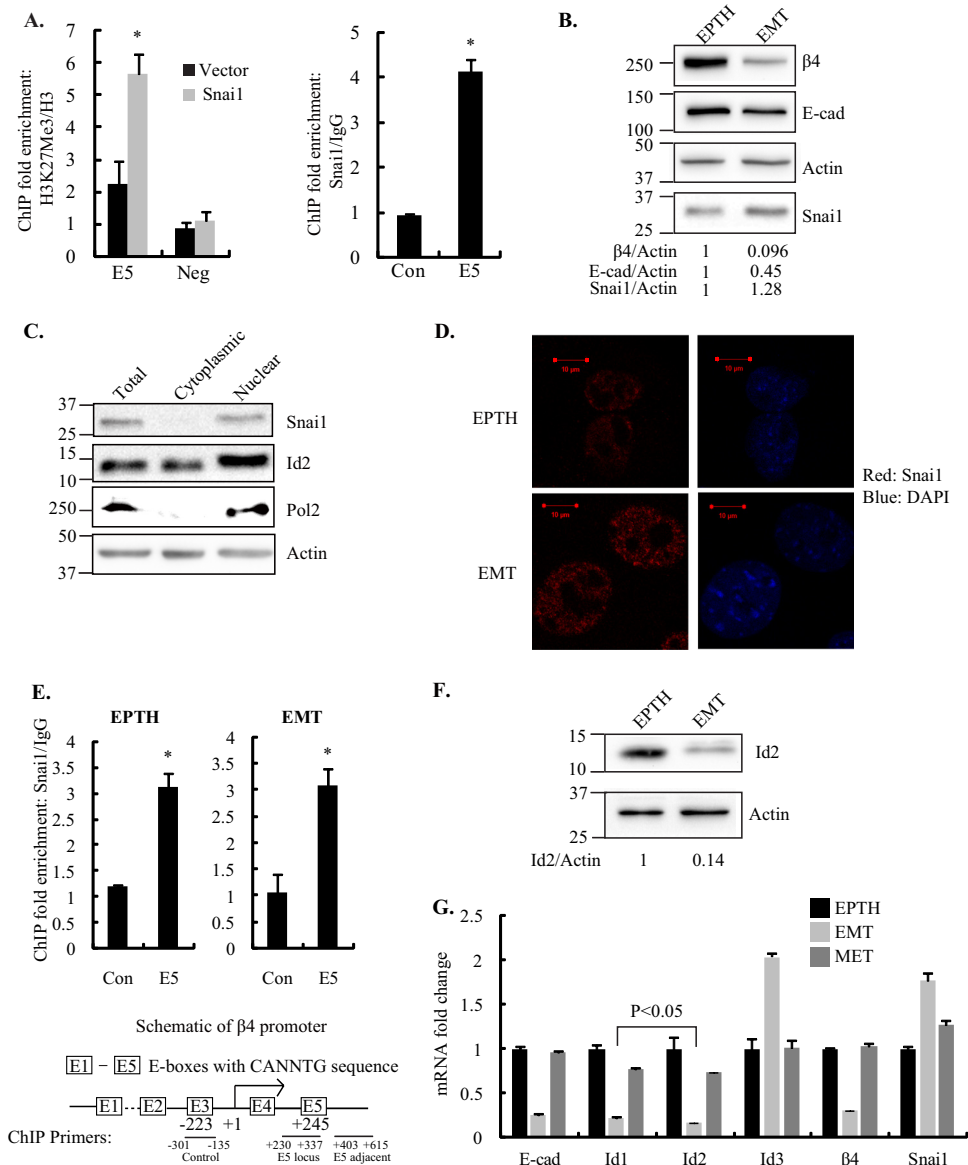
FIG 2 Nuclear Snai1 binds β4 promoter in epithelial cells. (A) NMuMG cells expressing Snai1 were generated, and the H3K27Me3 modification on β4 promoter was assessed using ChIP followed by qPCR (left); Snai1 binding on the β4 promoter in Snai1-expressing NMuMG cells was also assessed by ChIP followed by qPCR (right) (*, *P* < 0.05). The enrichment of the antibody was normalized to H3 (H3K27Me3) or IgG (Snai1). Con, control; Neg, negative. (B) NMuMG cells were treated with 4 ng/ml TGF-β (EMT) or vehicle (EPTH) for 2 days to induce an EMT, and the expression of β4, E-cadherin, actin, and Snai1 was assessed by immunoblotting. (C) Total cell extracts, as well as the cytoplasmic and nuclear fractions of epithelial NMuMG cells, were obtained. The expression of Snai1, Id2, Pol2 (positive control for the nucleus/negative control for the cytoplasm), and actin was assessed by immunoblotting. (D) The localization of Snai1 in control (EPTH) and TGF-β-treated (EMT) NMuMG cells was assessed by immunofluorescence using confocal microscopy. Scale bar, 10 μm. (E) Snai1 binding (top) on the β4 promoter in control (EPTH, left) and TGF-β-treated (EMT, right) NMuMG cells was determined by ChIP and qPCR (*, *P* < 0.05). The bottom panel shows a schematic of the β4 promoter, and the regions targeted by ChIP primers are indicated. Note that E5 includes E5 and the E5 adjacent locus, which are only 75 bp apart and below the resolution of ChIP (this is also the case in the following figures). (F) Extracts of control (EPTH) and TGF-β-treated (EMT) NMuMG cells were obtained, and the expression of Id2 and actin was assessed by immunoblotting. (G) NMuMG cells were treated with 4 ng/ml TGF-β (EMT) or vehicle (EPTH) for 3 days to induce an EMT, and then TGF-β was withdrawn for another 6 days to trigger an MET. Expression of β4, E-cadherin, Snai1, Id1, Id2, and Id3 mRNA was assessed by qPCR. Numbers on the left of the blots indicate the size (in kilodaltons) of the protein standard.

translation of Id1, Id2, and Snai1 was performed using a 1-Step Human *In Vitro* protein expression kit (ThermoFisher Scientific). The translated lysates were then precleared using 5 μl of a 50% suspension of GST beads prior to GST pulldown. Equal amounts of the GST fusion protein bead suspension were mixed with the *in vitro* translated lysates in the lysis buffer (20 mM Tris-HCl, pH 8.0, 200 mM NaCl, 1 mM EDTA, 0.5% NP-40, and protease inhibitor) with a total volume of 500 μl. After 2 h of

incubation at 4°C, the beads were washed four times with 1 ml of cold lysis buffer. Samples were resolved by SDS-PAGE and subjected to radioautography or immunoblotting. *In vitro* translated lysates (10 to 12%) were used as input.

Microarray data accession number. The microarray data have been deposited in the Gene Expression Omnibus (GEO) database under accession number GSE48204.
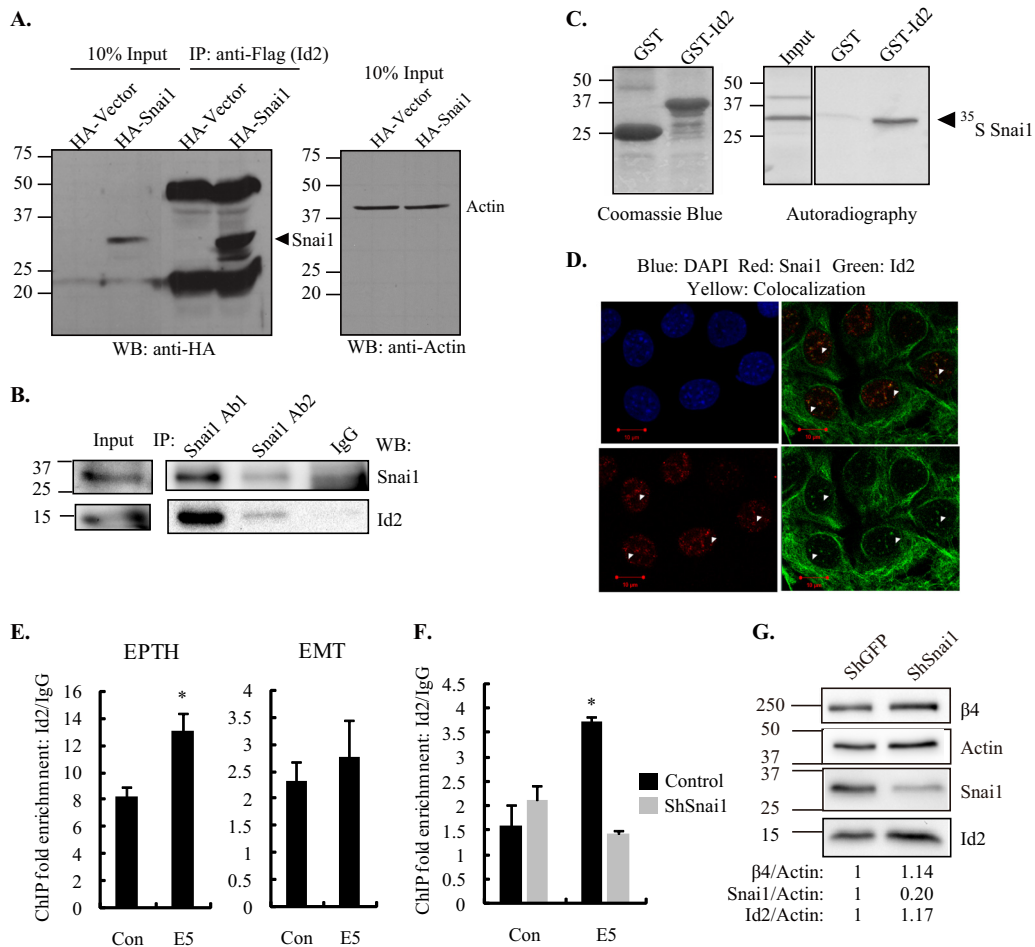
FIG 3 Id2 and Snai1 form a complex. (A) NMuMG cells were transiently cotransfected with pCMX-Flag-Id2 and pCMX-HA-Snai1/pCMX-HA for 72 h. Cell extracts were immunoprecipitated using anti-Flag beads and then immunoblotted using an HA Ab. Ten percent input was used as loading control. WB, Western blotting. (B) NMuMG extracts were immunoprecipitated using Snai1 Ab1 or Ab2 and blotted with Snai1 Ab1 and Id2. Total cell extract (10%) was run as a positive control (Input). (C) GST and GST-Id2 were expressed in *E. coli* and purified using glutathione-Sepharose beads. A fraction of the purified proteins was resolved by SDS-PAGE to verify the correct molecular mass of the target proteins (left). Subsequently, the *in vitro* transcribed/translated radioactive (^{35}S-methionine-labeled) Snai1 protein was subjected to GST pulldown by GST or GST-Id2, and the retained fraction or 10% input was resolved by SDS-PAGE and detected by radioautography (right). (D) The localization of Snai1 and Id2 in NMuMG cells was assessed by immunofluorescence using confocal microscopy. Scale bar, 10 μm. The arrowheads indicate sites of colocalization. (E and F) Id2 binding on the β4 promoter in control (EPTH) and TGF-β-treated (EMT) NMuMG cells (E) or in control and Snai1-depleted epithelial NMuMG cells (F) was assessed by ChIP followed by qPCR (*, $P < 0.05$). (G) The efficiency of Snai1 depletion in the experiment shown in panel F was assessed by immunoblotting. Numbers on the left of the blots indicate the size (in kilodaltons) of the protein standard.

RESULTS AND DISCUSSION

Snai1 represses integrin β4 transcription. The normal murine mammary gland cell line (NMuMG) undergoes a bona fide EMT in response to TGF-β, and subsequent TGF-β withdrawal results in a mesenchymal-epithelial transition (MET) (15, 33). To screen for potential factors that could repress β4 transcription, we compared the gene expression profiles of epithelial NMuMG cells (EPTH), TGF-β-treated NMuMG cells (EMT), and TGF-β treated/TGF-β withdrawn NMuMG cells (MET) (see Fig. S1A in the supplemental material). Among the potential EMT-promoting transcription factors, only Snai1 exhibited significant induction during EMT and reduction during MET (GEO accession number GSE48204).

Given that Snai1 can repress several epithelial genes including E-cadherin (18, 34–37), we assessed whether it could repress β4. For this purpose, we used an inducible system in

which a human Snai1 cDNA was fused with an estrogen receptor (ER) construct (29). This Snai1-ER construct was stably expressed in NMuMG cells, enabling Snai1 function to be activated in the presence of 4-hydroxytamoxifen (4-OHT). Activation of Snai1 activity repressed β4 protein and mRNA expression significantly (Fig. 1A and B). Note that 4-OHT itself had minimal effect on β4 expression and transcription in control cells. Expression of a mouse Snai1 cDNA in NMuMG cells also repressed β4 expression and transcription (Fig. 1C, D, and E). Snai1 also repressed E-cadherin expression (Fig. 1C), consistent with previous data (35, 36). Conversely, we diminished Snai1 expression using two independent shRNAs (Fig. 1F) and observed a rescue of β4 protein (Fig. 1G) and mRNA expression (Fig. 1H) in TGF-β-treated cells. Taken together, these data indicate that Snai1 represses β4 and is responsible for the loss of β4 during TGF-β-induced EMT.
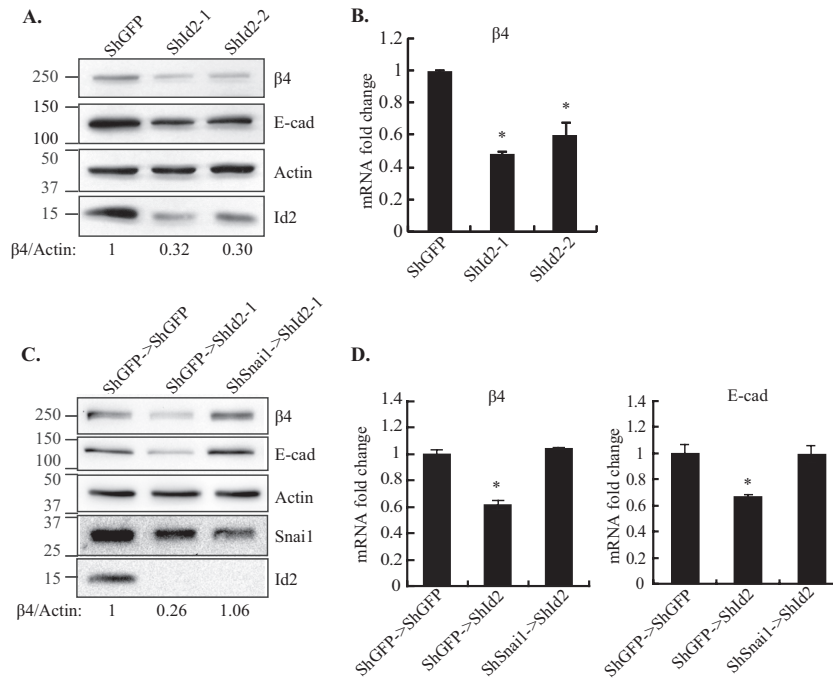
FIG 4 Repression of β4 as a consequence of Id2 loss is Snai1 dependent. (A) The expression of Id2 in NMuMG cells was diminished using two independent shRNAs, and the expression of β4, E-cadherin, Id2, and actin was examined by immunoblotting. (B) β4 mRNA expression in the cells described in panel A was quantified by qPCR (*, $P < 0.05$). (C) The expression of β4, E-cadherin, actin, Snai1, and Id2 was evaluated by immunoblotting in NMuMG cells that had been depleted of Id2 or both Id2 and Snai1 using shRNAs, and results were compared to levels in the appropriate shGFP control cells. (D) Expression of β4 and E-cadherin mRNAs in the cells described in panel C was quantified by qPCR (*, $P < 0.05$). Numbers on the left of the blots indicate the size (in kilodaltons) of the protein standard.

Snai1 induces the repressive histone mark H3K27Me3 on β4 promoter. Snai1 is known to modify the histone marks on the promoter of its target genes, including demethylation of H3K4 (38) and deacetylation of H3/H4 (39), as well as methylation of H3K27 (20), H3K9 (40, 41), and H4R3 (42). We chose to focus on the Polycomb complex-associated repressive mark, H3K27Me3, as a proof of principle for the function of Snai1 because our earlier study established that the increase of this mark is concomitant with the repression of β4 (15). Indeed, ectopic expression of Snai1 significantly increased the H3K27Me3 histone modification but not H3K9Me3 (see Fig. S1B in the supplemental material) on the β4 promoter, as evidenced by chromatin immunoprecipitation (ChIP) (Fig. 2A, left). This approach also demonstrated that Snai1 binds specifically to an E box that is located shortly after the transcription start site of the β4 promoter, designated E5 (Fig. 2A, right, and E, bottom for a schematic of the β4 promoter). Note that E5 is the only E box in the β4 promoter that is conserved across species (see Fig. S1C).

Snai1 is not functional in epithelial NMuMG cells. We detected Snai1 expression in epithelial NMuMG cells (Fig. 2B) and found that it is localized in the nucleus (Fig. 2C and D). This observation prompted us to use ChIP to assess the binding pattern of endogenous Snai1 on the β4 promoter in epithelial cells and compare it to EMT cells. Snai1 binds to the E5 in both epithelial and EMT cells (Fig. 2E). However, it does not repress β4 in epithelial NMuMG cells (Fig. 2B). Based on this observation, we speculated that an adaptor protein impedes the repressive function of Snai1 on E5. Id2 captured our attention for several reasons. Our microarray analysis (accession number GSE48204) revealed

that it is the most repressed gene during the EMT. Moreover, Id2 localized in both the nucleus and cytoplasm of epithelial cells (Fig. 2C), and its expression is depleted during the EMT (Fig. 2F and G). Id1 expression is also diminished during the EMT (Fig. 2G), but it has been reported to facilitate the EMT (43, 44). Interestingly, Id3 expression increases during the EMT (Fig. 2G).

Id2 and Snai1 form a complex. Although Id2 can interact with retinoblastoma protein (Rb) and basic HLH (bHLH) proteins (45–47), there is no evidence that it can complex with zinc finger proteins. To test the possibility that Snai1 partners with Id2, we performed coimmunoprecipitation assays and found that Id2 coimmunopurifies with Snai1 in vitro (Fig. 3A) and in vivo (Fig. 3B). Moreover, GST pulldown assays using Id2 as bait confirmed that this interaction is direct (Fig. 3C). These biochemical interactions were substantiated by the observation that Id2 and Snai1 colocalize in a punctate structure within the nuclei of epithelial NMuMG cells (Fig. 3D). Furthermore, ChIP experiments revealed that Id2 binds to the same locus (E5) of the β4 promoter as Snai1 does, and the binding is lost during the EMT (Fig. 3E). Importantly, knockdown of Snai1 diminished this specific enrichment of Id2 on the β4 promoter (Fig. 3F and G). Given that Id2 cannot bind DNA directly (45), these results indicate that an Snai1-Id2 complex binds to the β4 promoter in epithelial NMuMG cells.

Loss of Id2 diminishes β4 and E-cadherin expression. The finding that Id2 complexes with Snai1 in epithelial cells and that Snai1 does not repress β4 expression in these cells suggested that Id2 compromises the repressive function of Snai1. To disrupt this complex, we depleted Id2 by two independent shRNAs in epithelial cells and assessed β4 expression. Silencing Id2 resulted in de-
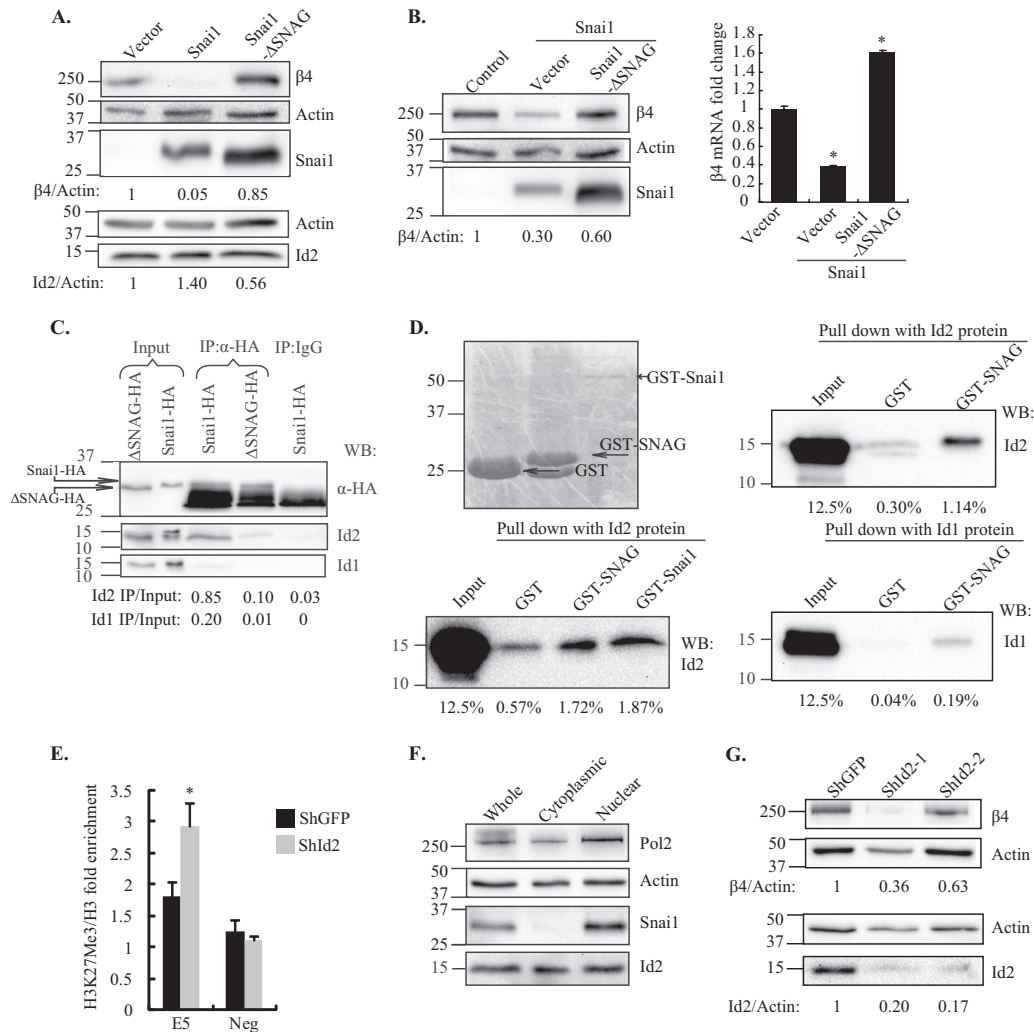
FIG 5 Id2 inhibits Snai1 by interacting with its SNAG domain. (A) NMuMG cells stably expressing either Snai1 or Snai1-ΔSNAG were generated, and the expression of β4, actin, and Snai1 was assessed by immunoblotting. (B) Ectopic expression of Snai1-ΔSNAG or vector in the cells stably expressing Snai1 was achieved by virus transduction. Subsequently, the expression of β4, actin, and Snai1 was assessed by immunoblotting (left). β4 mRNA expression in the same populations was quantified by qPCR (right) (*, $P < 0.05$). (C) Snai1-HA or Snai1-ΔSNAG-HA (referred to as ΔSNAG-HA) was expressed in NMuMG cells, and extracts were immunoprecipitated using HA antibody. The retained proteins were resolved by SDS-PAGE and subjected to immunoblotting. Ten percent input was used for each IP as a loading control. (D) GST, GST-SNAG, and GST-Snai1 constructs were expressed in *E. coli* and purified using glutathione-Sepharose beads. A fraction of the purified protein was resolved by SDS-PAGE to verify the molecular mass of the target proteins (upper). Subsequently, the *in vitro* transcribed/translated Id2 or Id1 protein was subjected to GST pulldown with either GST, GST-SNAG, or GST-Snai1 (as indicated on the figure), and the retained fraction or 12.5% of the input was resolved by SDS-PAGE and detected by immunoblotting (bottom). Numbers indicate the percentage of the pulled-down fraction relative to 100% input as determined by densitometry. (E) The H3K27Me3 modification on the β4 promoter in the Id2-depleted NMuMG cells was assessed by ChIP followed by qPCR (*, $P < 0.05$). (F) MCF7 cells were fractionated as described in the legend of Fig. 2C, and the expression of Id2, β4, Snai1, and Pol2 was assessed by immunoblotting. (G) Id2 expression was depleted in MCF7 cells using two independent shRNAs, and the expression of β4, actin, and Id2 in these cells, as well as in control cells, was assessed by immunoblotting. Numbers on the left of the blots/gels indicate the size (in kilodaltons) of the protein standard.

creased β4 mRNA and protein expression compared to levels in control cells (Fig. 4A and B). Importantly, knockdown of Snai1 in the Id2-silenced cells completely rescued the expression of β4 mRNA and protein, indicating that the repression of β4 that occurs in response to Id2 loss is Snai1 dependent (Fig. 4C and D). Similar results were obtained for E-cadherin, an established target of Snai1 (Fig. 4A, C, and D). Taken together, these data reveal that Id2 restrains Snai1 from its ability to repress epithelial genes.

Id2 masks the SNAG domain of Snai1 and prevents the H3K27Me3 repressive mark. The SNAG domain is crucial for the

repressive function of Snai1 because it mediates the interaction of Snai1 with many corepressors (20, 38, 39, 41). This finding is consistent with our data that deletion of this domain abrogated the ability of Snai1 to repress β4 expression (Fig. 5A). Moreover, a ΔSNAG mutant of Snai1 functions as a dominant negative mutant that rescues β4 expression in NMuMG cells engineered to express Snai1 (Fig. 5B). Given the importance of this domain and our observation that Id2 inhibits the function of Snai1 via a complex formation, the possibility emerged that the Id2-Snai1 interaction is mediated through the SNAG domain of Snai1. Indeed, HA-
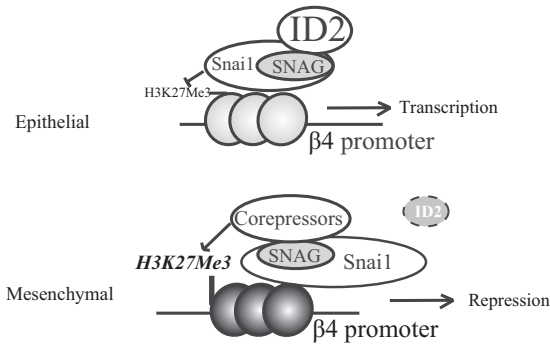
FIG 6 Proposed model of how Id2 regulates Snail-mediated repression of integrin β4. Id2 complexes with the SNAG domain of Snai1 bind to the β4 promoter in epithelial cells, and it impairs the ability of Snai1 to increase the trimethylation of H3K27 on the β4 promoter. The loss of Id2 that occurs as a consequence of the EMT enables putative corepressors to increase H3K27Me3 and represses β4 transcription.

Snai1 coimmunopurified with Id2, but the HA-ΔSNAG mutant failed to do so (Fig. 5C), demonstrating that SNAG is essential for the Id2-Snai1 interaction. Moreover, we confirmed that the SNAG domain itself is sufficient to bind Id2 directly using a GST-pulldown approach, in which the GST-SNAG domain fusion protein was used as bait for Id2 (Fig. 5D). Considering that Id1 is also repressed by the EMT (Fig. 2G), we also examined the potential interaction between Id1 and Snai1 in the same setting. Although Id1 and Snai1 can interact, the interaction is 4- to 6-fold weaker than the interaction between Id2 and Snai1 (Fig. 5C and D). This finding indicates that that Id2 is a dominant interacting partner of Snai1 when both Id1 and Id2 are expressed.

Our data indicate that Id2 can mask the SNAG domain, which should result in the failure of Snai1 to establish H3K27Me3. Indeed, knockdown of Id2 in epithelial NMuMG cells caused a significant elevation of this repressive histone mark (Fig. 5E). We also assessed whether Id2-Snai1-mediated regulation of β4 occurs in other epithelial cells. Specifically, MCF7 cells are well-differentiated carcinoma cells that express β4, Id2, and Snai1 (Fig. 5F and G). Importantly, endogenous Snai1 is localized in the nucleus of these cells (Fig. 5F), and knockdown of Id2 caused a reduction of β4 expression (Fig. 5G).

A major conclusion of our study is that Snai1 can be expressed in the nucleus of epithelial cells and bind to specific promoters, but its ability to repress transcription is restrained by its association with Id2 (Fig. 6). More specifically, we demonstrate that the repressive function of Snai1 is compromised by the interaction of its SNAG domain with Id2. To our knowledge, this is the first identification of a functional antagonist that binds the SNAG domain of Snai1 in the epithelial cells. In previous studies, the SNAG domain was shown to be essential for recruiting several cooperative cofactors that are necessary for removing active histone marks and adding repressive ones, including Suz12 (20), Suv39H1 (41), LSD1 (38), HDAC1/2 (39), and Ezh2 (48). Based on our observation that the repressive mark H3K27Me3, but not H3K9Me3, is elevated in response to Id2 loss, it is possible that the corepressor responsible for H3K27Me3, Ezh2, is unable to bind Snai1 in the presence of Id2. We pursued this possibility experimentally, but the data generated did not enable a definitive conclusion.

The ability of Id2 to complex with the zinc finger protein Snai1 provides a novel mechanism accounting for the role of Id2 in the EMT. It is known that Id2 is repressed dramatically in epithelial cells by TGF-β signaling and that forced expression of Id2 rescues epithelial gene expression in TGF-β-treated cells (21). The ability of Id2 to bind and sequester E2A, a basic helix-loop-helix protein, from binding target genes including E-cadherin has been proposed as a mechanism to account for these observations (22). Our finding that Id2 complexes with Snai1 on the promoter of the target gene and prevents Snai1 from recruiting transcriptional corepressors provides a distinct mechanism for how Id2 contributes to epithelial differentiation. Collectively, the existing data substantiate the potency of Snai1 in promoting a mesenchymal transition and its need to be regulated. Our finding that Id1 can also interact with Snai1 suggests that this interaction may involve the HLH domain. Given that the interaction with Id2 is much stronger than Id2, Id2-specific domains may also be involved in Id2-Snai1 association.

The data reported here expand and complement other studies on the repression of β4 and other epithelial genes. Snail has a preeminent role in the repression of β4 (Fig. 1) and E-cadherin (36), but several other factors contribute to this repression, including Twist, Slug, and Zeb1 (13). For example, based on the findings that Zeb1 represses β4 transcription (49) and that Snai1 induces Zeb1 expression (50), we infer that β4 transcriptional repression involves a cascade of Snai1- and Zeb1-mediated events and that Id2 functions upstream to prevent the initiation of this cascade by complexing with the SNAG domain of Snai1. This hypothesis is supported by the observation that Id2 overexpression in TGF-β-treated epithelial cells suppressed Zeb1 induction (51). In a different direction, we reported that β4 repression during the EMT is associated with promoter methylation (15), and it is known that Snai1 can mediate DNA methylation (40). Although these observations suggest that methylation of the β4 promoter should increase in response to Id2 loss, we did not detect such an increase (data not shown). Most likely, this observation indicates that additional factors are required for *de novo* methylation, such as DNMT3s (52).

The mechanistic relationship between Id2 and β4 is foreshadowed by other studies that support our central hypothesis. Of note, the progenitor population of lung epithelial cells is enriched in both Id2 and β4 expression (53, 54), suggesting that Id2 may facilitate the purported role of β4 in the function of lung epithelial stem cells (55). Our data may also have significant implications for the regulation of β4 in cancer. For example, nuclear Id2 expression correlates significantly with a poor prognosis in non-small-cell lung carcinoma (56), and β4 expression is also upregulated in these carcinomas (57). Clearly, Id2-mediated regulation of β4 expression merits further investigation, especially in the context of metastasis, which involves a reversion to an epithelial phenotype and increased expression of β4 (58).

REFERENCES

1. **Hynes RO.** 2002. Integrins: bidirectional, allosteric signaling machines. Cell **110:**673–687.
2. **Yurchenco PD.** 2011. Basement membranes: cell scaffoldings and signal-

ing platforms. Cold Spring Harb. Perspect. Biol. **3**:a004911. doi:10.1101/cshperspect.a004911.

3. **Stepp MA, Zhu L, Cranfill R.** 1996. Changes in beta 4 integrin expression and localization in vivo in response to corneal epithelial injury. Invest. Ophthalmol. Vis. Sci. **37**:1593–1601.

4. **Margadant C, Sonnenberg A.** 2010. Integrin-TGF-beta crosstalk in fibrosis, cancer and wound healing. EMBO Rep. **11**:97–105.

5. **Lipscomb EA, Mercurio AM.** 2005. Mobilization and activation of a signaling competent α6β4 integrin underlies its contribution to carcinoma progression. Cancer Metastasis Rev. **24**:413–423.

6. **DiPersio CM, Hodivala-Dilke KM, Jaenisch R, Kreidberg JA, Hynes RO.** 1997. α3β1 Integrin is required for normal development of the epidermal basement membrane. J. Cell Biol. **137**:729–742.

7. **Stepp MA, Spurr-Michaud S, Tisdale A, Elwell J, Gipson IK.** 1990. α6β4 integrin heterodimer is a component of hemidesmosomes. Proc. Natl. Acad. Sci. U. S. A. **87**:8970–8974.

8. **Watt FM.** 2002. Role of integrins in regulating epidermal adhesion, growth and differentiation. EMBO J. **21**:3919–3926.

9. **Lee EC, Lotz MM, Steele GD, Jr., Mercurio AM.** 1992. The integrin α6β4 is a laminin receptor. J. Cell Biol. **117**:671–678.

10. **Rabinovitz I, Mercurio AM.** 1997. The integrin α6β4 functions in carcinoma cell migration on laminin-1 by mediating the formation and stabilization of actin-containing motility structures. J. Cell Biol. **139**:1873–1884.

11. **Rabinovitz I, Toker A, Mercurio AM.** 1999. Protein kinase C-dependent mobilization of the α6β4 integrin from hemidesmosomes and its association with actin-rich cell protrusions drive the chemotactic migration of carcinoma cells. J. Cell Biol. **146**:1147–1160.

12. **Mercurio AM, Rabinovitz I, Shaw LM.** 2001. The α6β4 integrin and epithelial cell migration. Curr. Opin. Cell Biol. **13**:541–545.

13. **Thiery JP, Acloque H, Huang RY, Nieto MA.** 2009. Epithelial-mesenchymal transitions in development and disease. Cell **139**:871–890.

14. **Yang J, Weinberg RA.** 2008. Epithelial-mesenchymal transition: at the crossroads of development and tumor metastasis. Dev. Cell **14**:818–829.

15. **Yang X, Pursell B, Lu S, Chang TK, Mercurio AM.** 2009. Regulation of beta 4-integrin expression by epigenetic modifications in the mammary gland and during the epithelial-to-mesenchymal transition. J. Cell Sci. **122**:2473–2480.

16. **Putzke AP, Ventura AP, Bailey AM, Akture C, Opoku-Ansah J, Celiktas M, Hwang MS, Darling DS, Coleman IM, Nelson PS, Nguyen HM, Corey E, Tewari M, Morrissey C, Vessella RL, Knudsen BS.** 2011. Metastatic progression of prostate cancer and E-cadherin regulation by Zeb1 and SRC family kinases. Am. J. Pathol. **179**:400–410.

17. **Celia-Terrassa T, Meca-Cortes O, Mateo F, de Paz AM, Rubio N, Arnal-Estape A, Ell BJ, Bermudo R, Diaz A, Guerra-Rebollo M, Lozano JJ, Estaras C, Ulloa C, Alvarez-Simon D, Mila J, Vilella R, Paciucci R, Martinez-Balbas M, de Herreros AG, Gomis RR, Kang Y, Blanco J, Fernandez PL, Thomson TM.** 2012. Epithelial-mesenchymal transition can suppress major attributes of human epithelial tumor-initiating cells. J. Clin. Invest. **122**:1849–1868.

18. **Vincent T, Neve EP, Johnson JR, Kukalev A, Rojo F, Albanell J, Pietras K, Virtanen I, Philipson L, Leopold PL, Crystal RG, de Herreros AG, Moustakas A, Pettersson RF, Fuxe J.** 2009. A SNAIL1-SMAD3/4 transcriptional repressor complex promotes TGF-beta mediated epithelial-mesenchymal transition. Nat. Cell Biol. **11**:943–950.

19. **Zhou BP, Deng J, Xia W, Xu J, Li YM, Gunduz M, Hung MC.** 2004. Dual regulation of Snail by GSK-3β-mediated phosphorylation in control of epithelial-mesenchymal transition. Nat. Cell Biol. **6**:931–940.

20. **Herranz N, Pasini D, Diaz VM, Franci C, Gutierrez A, Dave N, Escriva M, Hernandez-Munoz I, Di Croce L, Helin K, Garcia de Herreros A, Peiro S.** 2008. Polycomb complex 2 is required for E-cadherin repression by the Snail1 transcription factor. Mol. Cell. Biol. **28**:4772–4781.

21. **Kowanetz M, Valcourt U, Bergstrom R, Heldin CH, Moustakas A.** 2004. Id2 and Id3 define the potency of cell proliferation and differentiation responses to transforming growth factor beta and bone morphogenetic protein. Mol. Cell. Biol. **24**:4241–4254.

22. **Kondo M, Cubillo E, Tobiume K, Shirakihara T, Fukuda N, Suzuki H, Shimizu K, Takehara K, Cano A, Saitoh M, Miyazono K.** 2004. A role for Id in the regulation of TGF-beta-induced epithelial-mesenchymal transdifferentiation. Cell Death Differ. **11**:1092–1101.

23. **Affymetrix.** 2008. 3′ IVT Express Kit user manual. Affymetrix, Santa Clara, CA.

24. **Simon R, Lam A, Li MC, Ngan M, Menenzes S, Zhao Y.** 2007. Analysis of gene expression data using BRB-ArrayTools. Cancer Inform. **3**:11–17.

25. **Shaw LM, Rabinovitz I, Wang HH, Toker A, Mercurio AM.** 1997. Activation of phosphoinositide 3-OH kinase by the α6β4 integrin promotes carcinoma invasion. Cell **91**:949–960.

26. **Littlewood TD, Hancock DC, Danielian PS, Parker MG, Evan GI.** 1995. A modified oestrogen receptor ligand-binding domain as an improved switch for the regulation of heterologous proteins. Nucleic Acids Res. **23**:1686–1690.

27. **Metzger D, Clifford J, Chiba H, Chambon P.** 1995. Conditional site-specific recombination in mammalian cells using a ligand-dependent chimeric Cre recombinase. Proc. Natl. Acad. Sci. U. S. A. **92**:6991–6995.

28. **Danielian PS, White R, Hoare SA, Fawell SE, Parker MG.** 1993. Identification of residues in the estrogen receptor that confer differential sensitivity to estrogen and hydroxytamoxifen. Mol. Endocrinol. **7**:232–240.

29. **Mani SA, Guo W, Liao MJ, Eaton EN, Ayyanan A, Zhou AY, Brooks M, Reinhard F, Zhang CC, Shipitsin M, Campbell LL, Polyak K, Brisken C, Yang J, Weinberg RA.** 2008. The epithelial-mesenchymal transition generates cells with properties of stem cells. Cell **133**:704–715.

30. **Tian B, Yang J, Brasier AR.** 2012. Two-step cross-linking for analysis of protein-chromatin interactions. Methods Mol. Biol. **809**:105–120.

31. **Franci C, Takkunen M, Dave N, Alameda F, Gomez S, Rodriguez R, Escriva M, Montserrat-Sentis B, Baro T, Garrido M, Bonilla F, Virtanen I, Garcia de Herreros A.** 2006. Expression of Snail protein in tumor-stroma interface. Oncogene **25**:5134–5144.

32. **Einarson MB, Pugacheva EN, Orlinick JR.** 2007. GST Pull-down. CSH Protoc. **2007**:pdb.prot4757. doi:10.1101/pdb.prot4757.

33. **Gal A, Sjoblom T, Fedorova L, Imreh S, Beug H, Moustakas A.** 2008. Sustained TGFβ exposure suppresses Smad and non-Smad signalling in mammary epithelial cells, leading to EMT and inhibition of growth arrest and apoptosis. Oncogene **27**:1218–1230.

34. **Guaita S, Puig I, Franci C, Garrido M, Dominguez D, Batlle E, Sancho E, Dedhar S, De Herreros AG, Baulida J.** 2002. Snail induction of epithelial to mesenchymal transition in tumor cells is accompanied by MUC1 repression and ZEB1 expression. J. Biol. Chem. **277**:39209–39216.

35. **Batlle E, Sancho E, Franci C, Dominguez D, Monfar M, Baulida, J Garcia De Herreros A.** 2000. The transcription factor snail is a repressor of E-cadherin gene expression in epithelial tumour cells. Nat. Cell Biol. **2**:84–89.

36. **Cano A, Perez-Moreno MA, Rodrigo I, Locascio A, Blanco MJ, del Barrio MG, Portillo F, Nieto MA.** 2000. The transcription factor snail controls epithelial-mesenchymal transitions by repressing E-cadherin expression. Nat. Cell Biol. **2**:76–83.

37. **Vega S, Morales AV, Ocana OH, Valdes F, Fabregat I, Nieto MA.** 2004. Snail blocks the cell cycle and confers resistance to cell death. Genes Dev. **18**:1131–1143.

38. **Lin Y, Wu Y, Li J, Dong C, Ye X, Chi YI, Evers BM, Zhou BP.** 2010. The SNAG domain of Snail1 functions as a molecular hook for recruiting lysine-specific demethylase 1. EMBO J. **29**:1803–1816.

39. **Peinado H, Ballestar E, Esteller M, Cano A.** 2004. Snail mediates E-cadherin repression by the recruitment of the Sin3A/histone deacetylase 1 (HDAC1)/HDAC2 complex. Mol. Cell. Biol. **24**:306–319.

40. **Dong C, Wu Y, Yao J, Wang Y, Yu Y, Rychahou PG, Evers BM, Zhou BP.** 2012. G9a interacts with Snail and is critical for Snail-mediated E-cadherin repression in human breast cancer. J. Clin. Invest. **122**:1469–1486.

41. **Dong C, Wu Y, Wang Y, Wang C, Kang T, Rychahou PG, Chi YI, Evers BM, Zhou BP.** 2013. Interaction with Suv39H1 is critical for Snail-mediated E-cadherin repression in breast cancer. Oncogene **32**:1351–1362.

42. **Hou Z, Peng H, Ayyanathan K, Yan KP, Langer EM, Longmore GD, and Rauscher FJ, III.** 2008. The LIM protein AJUBA recruits protein arginine methyltransferase 5 to mediate SNAIL-dependent transcriptional repression. Mol. Cell. Biol. **28**:3198–3207.

43. **Cheung PY, Yip YL, Tsao SW, Ching YP, Cheung AL.** 2011. Id-1 induces cell invasiveness in immortalized epithelial cells by regulating cadherin switching and Rho GTPases. J. Cell. Biochem. **112**:157–168.

44. **Cubillo E, Diaz-Lopez A, Cuevas EP, Moreno-Bueno G, Peinado H, Montes A, Santos V, Portillo F, Cano A.** 2013. E47 and Id1 interplay in epithelial-mesenchymal transition. PLoS One **8**:e59948. doi:10.1371/journal.pone.0059948.

45. **Norton JD.** 2000. ID helix-loop-helix proteins in cell growth, differentiation and tumorigenesis. J. Cell Sci. **113**:3897–3905.

46. **Benezra R, Davis RL, Lockshon D, Turner DL, Weintraub H.** 1990. The protein Id: a negative regulator of helix-loop-helix DNA binding proteins. Cell **61:**49–59.

47. **Iavarone A, Garg P, Lasorella A, Hsu J, Israel MA.** 1994. The helix-loop-helix protein Id-2 enhances cell proliferation and binds to the retinoblastoma protein. Genes Dev. **8:**1270–1284.

48. **Tong ZT, Cai MY, Wang XG, Kong LL, Mai SJ, Liu YH, Zhang HB, Liao YJ, Zheng F, Zhu W, Liu TH, Bian XW, Guan XY, Lin MC, Zeng MS, Zeng YX, Kung HF, Xie D.** 2012. EZH2 supports nasopharyngeal carcinoma cell aggressiveness by forming a co-repressor complex with HDAC1/HDAC2 and Snail to inhibit E-cadherin. Oncogene **31:**583–594.

49. **Drake JM, Barnes JM, Madsen JM, Domann FE, Stipp CS, Henry MD.** 2010. ZEB1 coordinately regulates laminin-332 and β4 integrin expression altering the invasive phenotype of prostate cancer cells. J. Biol. Chem. **285:**33940–33948.

50. **Dave N, Guaita-Esteruelas S, Gutarra S, Frias A, Beltran M, Peiro S, de Herreros AG.** 2011. Functional cooperation between Snail1 and twist in the regulation of ZEB1 expression during epithelial to mesenchymal transition. J. Biol. Chem. **286:**12024–12032.

51. **Shirakihara T, Saitoh M, Miyazono K.** 2007. Differential regulation of epithelial and mesenchymal markers by δEF1 proteins in epithelial mesenchymal transition induced by TGF-β. Mol. Biol. Cell **18:**3533–3544.

52. **Cedar H, Bergman Y.** 2009. Linking DNA methylation and histone modification: patterns and paradigms. Nat. Rev. Genet. **10:**295–304.

53. **Rawlins EL, Clark CP, Xue Y, Hogan BL.** 2009. The Id2+ distal tip lung epithelium contains individual multipotent embryonic progenitor cells. Development **136:**3741–3745.

54. **McQualter JL, Yuen K, Williams B, Bertoncello I.** 2010. Evidence of an epithelial stem/progenitor cell hierarchy in the adult mouse lung. Proc. Natl. Acad. Sci. U. S. A. **107:**1414–1419.

55. **Chapman HA, Li X, Alexander JP, Brumwell A, Lorizio W, Tan K, Sonnenberg A, Wei Y, Vu TH.** 2011. Integrin α6β4 identifies an adult distal lung epithelial population with regenerative potential in mice. J. Clin. Invest. **121:**2855–2862.

56. **Rollin J, Blechet C, Regina S, Tenenhaus A, Guyetant S, Gidrol X.** 2009. The intracellular localization of ID2 expression has a predictive value in non small cell lung cancer. PLoS One **4:**e4158. doi:10.1371/journal.pone.0004158.

57. **Boelens MC, van den Berg A, Vogelzang I, Wesseling J, Postma DS, Timens W, Groen HJ.** 2007. Differential expression and distribution of epithelial adhesion molecules in non-small cell lung cancer and normal bronchus. J. Clin. Pathol. **60:**608–614.

58. **Falcioni R, Kennel SJ, Giacomini P, Zupi G, Sacchi A.** 1986. Expression of tumor antigen correlated with metastatic potential of Lewis lung carcinoma and B16 melanoma clones in mice. Cancer Res. **46:**5772–5778.